HAL open science

Analysis of a Fully Packed Loop Model Arising in a Magnetic Coulomb Phase

L. D. C. Jaubert, M. Haque, R. Moessner

▶ To cite this version:

L. D. C. Jaubert, M. Haque, R. Moessner. Analysis of a Fully Packed Loop Model Arising in a Magnetic Coulomb Phase. Physical Review Letters, 2011, 107, pp.177202. 10.1103/PhysRevLett.107.177202 . hal-01541713

HAL Id: hal-01541713

https://hal.science/hal-01541713v1

Submitted on 19 Jun 2017

HAL is a multi-disciplinary open access archive for the deposit and dissemination of scientific research documents, whether they are published or not. The documents may come from teaching and research institutions in France or abroad, or from public or private research centers.

L'archive ouverte pluridisciplinaire **HAL**, est destinée au dépôt et à la diffusion de documents scientifiques de niveau recherche, publiés ou non, émanant des établissements d'enseignement et de recherche français ou étrangers, des laboratoires publics ou privés.

Distributed under a Creative Commons Attribution 4.0 International License

Analysis of a fully packed loop model arising in a magnetic Coulomb phase

L. D. C. Jaubert, M. Haque, and R. Moessner
Max-Planck-Institut für Physik komplexer Systeme, 01187 Dresden, Germany.
(Dated: March 29, 2011)

The Coulomb phase of spin ice, and indeed the I_c phase of water ice, naturally realise a fully-packed two-colour loop model in three dimensions. We present a detailed analysis of the statistics of these loops, which avoid themselves and other loops of the same colour, and contrast their behaviour to an analogous two-dimensional model. The properties of another extended degree of freedom are also addressed, flux lines of the emergent gauge field of the Coulomb phase, which appear as "Dirac strings" in spin ice. We mention implications of these results for related models, and experiments.

arXiv:1103.5397v1 [cond-mat.stat-mech] 28 Mar 2011

Introduction: In the study of magnetism, we are naturally led to consider local degrees of freedom and their correlations, such as the long-range order of the local spin orientation in a ferromagnet. In other settings, the fundamental degrees of freedom are extended, with polymers presenting perhaps the most familiar instance.

In magnets in two dimensions (2D), linearly extended objects do occur in the form of magnetic domain walls. The study of such 'non-local' degrees of freedom, involving questions such as: "What is the probability for two bonds to be on the same domain wall?", is related to problems like the geometry of the hull of a percolating cluster. Some beautiful theories have been developed in this context [1–3]. The same questions in higher dimension do not lend themselves to similarly exact approaches, but fractal extended objects in 3D have been studied in the contexts of polymer physics [4], cosmic strings [5, 6], magnetic filaments in manganite materials [7], and laser speckles [8].

Here, we discuss a 3D frustrated magnetic system, spin ice [9], exhibiting *two distinct* extended degrees of freedom, which we call loops and worms. Spin ice is unusual in that its low-temperature magnetic state is neither ordered (as in a ferromagnet) nor disordered (as in a paramagnet). Rather, this state is a *Coulomb phase*, where an emergent conservation law leads to algebraic spin correlations at low temperatures [10]. This has recently been confirmed experimentally for the compound $Ho_2Ti_2O_7$ [11]. The loops define a two-color fully packed loop model on the diamond lattice (the "premedial" lattice of the pyrochlore [12]), and they also appear in models for pyrochlore compounds with two species of magnetic ions [12–14] or itinerant electrons subject to double exchange [15]. Worms, named after their appearance in Monte Carlo worm algorithms [16], only come in one flavour and can pass through themselves and each other. They play a conceptually important role in the physics of spin ice as they are connected to "Dirac strings" and deconfinement in the Coulomb phase [17, 18]. Thus, besides their interest in the statistical mechanics of lattice models, we study loops and worms to elucidate the properties of this new magnetic phase.

In this paper, we numerically evaluate fundamental characteristics such as the probability distribution function (PDF) of loop length ℓ, radius of gyration and the probability for two sites separated by distance r to be on the same loop, $C(r)$. We present analytical arguments to account for the observed regimes and their concomitant power laws, and contrast this behaviour to the analogous model in two dimensions, on the checkerboard (Fig. 1), whose premedial lattice is the square lattice. Finally, we mention possible experimental signatures and touch on related models which naturally occur in the study of frustrated magnets and multi-colored loop models [12, 13].

Loops and worms: In spin ice, classical Ising spins live on the sites of the pyrochlore, or equivalently, the bonds of the diamond lattice. At low temperature, an exponentially large number of degenerate ground state configurations is available, $\exp(NS_p)$, where N is the number of spins and $S_p = \frac{1}{2}\log\frac{3}{2}$ is Pauling's ice entropy. These states obey the ice rules, stating that two of the bonds emanating from a diamond lattice site are occupied by up spins, the other two by down spins. They correspond to the allowed configurations of cubic ice I_c, captured by the six-vertex model on the diamond lattice. The ensemble of these states provides the Coulomb phase exhibiting an emergent gauge field and algebraic correlations [10, 12].

By coloring the links occupied by up and down spins differently, we obtain a fully packed (each link hosts a loop segment) two-color loop model. In contrast, a worm contains an alternating sequence of adjacent up and down spins (Fig. 1). There are different possible constructions for a worm. We adopt an unbiased one in which a worm, having entered a tetrahedron, exits through one of the two opposite spins in that tetrahedron with equal probability. A worm ends when it meets its initital site.

We consider periodic systems of square or cubic geometry with L unit cells in each direction, so that there are $N = 4L^2$ and $N = 16L^3$ lattice sites for the checkerboard and pyrochlore cases respectively. The smallest possible loop is $\ell_{min} = 4$ (6) for checkerboard (pyrochlore). We denote by $\langle\ell\rangle$ the average loop length and use subscripts c or $2d$ (p or $3d$) for checkerboard (pyrochlore).

Loop length distributions: Fig. 2 presents the PDF of the loop length obtained using the Monte Carlo worm algorithm [16]. For the checkerboard, the PDF has a single power-law behavior, $P_{2d} \sim \ell^{-\tau_c}$, with $\tau_c = 2.14(1)$. For related models (*sans* ice rules), this quantity is known

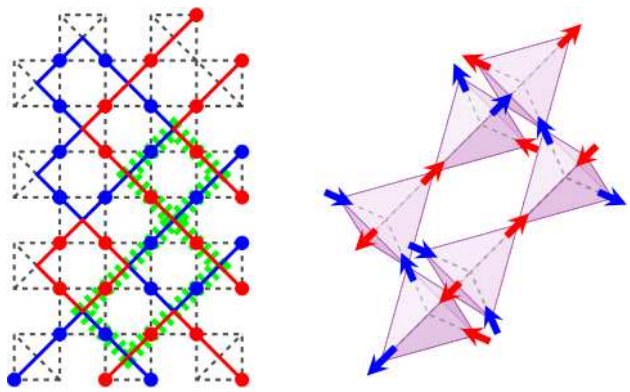

FIG. 1: *Left:* Loops of two colors, blue (red) for up (down) spins, and a worm (dashed green, made of alternating up and down spins), on the checkerboard lattice. The way we have drawn the loops highlights the fact that they fully occupy the premedial square lattice. A worm can cross itself and retrace its path. *Right:* Spin Ice model on the pyrochlore lattice with in (blue) and out (red) spins.

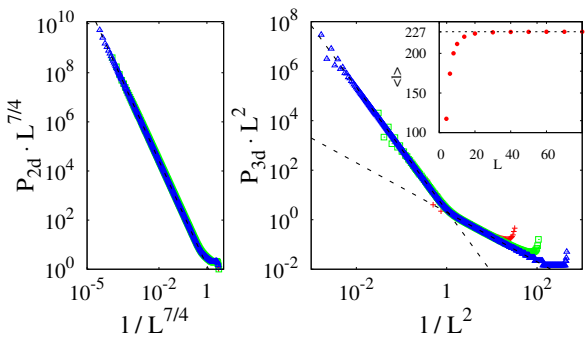

FIG. 2: Probability distribution functions of loop lengths ℓ on the checkerboard (left) and pyrochlore (right) lattice, for different system sizes (L = 100, 400, 1000 in 2D and L = 4, 14, 60 in 3D). Each axis is scaled by a power of L. Note the absence of one-parameter scaling in 3D at large ℓ. *Inset:* Average loop length on the pyrochlore lattice, converging with system size to a finite value of 227.3 (dashed line).

exactly to be $\tau_c = 2+1/7$ (Ref. [3] and Refs. thereof). No such exact value is available for τ_p. In fact, the situation for the 3D pyrochlore is dramatically different. There are now two different power-law regions: a short loop region where the PDF scales as $\sim L^3\ell^{-2.50(1)}$, and then a crossover at $\ell_1 \sim L^2$ to a large-ℓ region with scaling $\sim \ell^{-0.98(3)}$. The second regime is due to the influence of *winding loops*, which close only after crossing the periodic boundaries. We have checked that the PDF of only non-winding loops has a single power law, $\sim L^3\ell^{-5/2}$. In 2D, the loop distribution is dominated by non-winding loops at all ℓ. This is reminiscent of Pólya's theorem, that a random walk in 2D is *recurrent* (always returns to the initial point), while in 3D it is *transient* (a finite probability never to return) [19]. In both 2D and 3D, $P(\ell)$ briefly increases just before the cutoff at large ℓ.

Winding and non-winding loop fractions: In 2D, the average number of winding loops is 1.86(1) for large L. In contrast, in the pyrochlore this number scales as $N_{\rm w} \sim \ln L$. In both cases the number of non-winding loop scales as the total number of sites. In the large-L limit, the percentage of pyrochlore sites belonging to non-winding and winding loops are 6.310(5)% and 93.690(5)% respectively. Thus a finite but small portion of the system is covered by an extensive number of short loops, while most of the lattice sites belong to a few large loops.

Probability to be on the same loop: In 2D, we find $C(r)\sim r^{-1/2}$, in analogy with [3]. By contrast, in 3D, the leading term in $C(r)$ is a constant (Fig. 3), i.e. sites far from each other have a nonzero probability to be on the same loop. This is another qualitatively new feature of the 3D case arising from the transient nature of 3D loops.

Radius of gyration: This is defined as $R^2 = \frac{1}{\ell}\sum_{i=1}^{\ell} |\mathbf{r}_i - \langle \mathbf{r} \rangle|^2$ where $\mathbf{r}_i$ is the position of the ith site of the loop of length ℓ and $\langle \mathbf{r} \rangle = \sum_i \mathbf{r}_i/\ell$. This follows a power law $R \sim \ell^{\nu}$. We find $\nu = 0.573(5)$ in 2D, consistent with 4/7 [3]. In 3D, we find $\nu = 0.500(5)$. This is the value for the random walk rather than the self-avoiding ($\nu \approx 3/5$) walk, even though our loops are self-avoiding. This is similar in spirit to the observation for *dense* polymer solutions [4], that the need to avoid other loops counteracts the effects of self-avoidance.

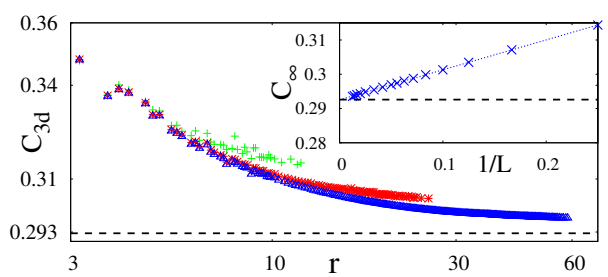

FIG. 3: Probability for two spins to be on the same loop as a function of the distance between them, on pyrochlore lattices with L = 4, 8, 18, asymptoting to $C_\infty = 0.2926(10)$ (dashed lines), found by an extrapolation to large system sizes (inset).

Ideal-chain analogy: We next present an analysis which accounts for the above results by applying known results from the theory of random walks (ideal chains) to this setting. The probability for an ideal chain starting at $\mathbf{x_o}$, to visit position $\mathbf{x}$ after ℓ steps, is $p(\mathbf{x_o}, \mathbf{x}; \ell) = (2\pi\ell)^{-3/2} e^{-(\mathbf{x}-\mathbf{x_o})^2/2\ell}$, in the 3D continuum [19]. Thus, the probability to come back to the initial point is $p(\mathbf{x_o}; \ell) = (2\pi\ell)^{-3/2}$. Summing over all possible starting positions, one obtains the following loop length PDF for non-winding loops:

$$P_{3d}^{\rm nw}(\ell) \approx \frac{1}{\ell}\sum_{\mathbf{x}_o} p(\mathbf{x_o};\ell) \sim L^3\ell^{-5/2} \qquad (1)$$

where the factor $1/\ell$ compensates the arbitrariness in defining the starting position along the loop of size ℓ.

To understand the different exponent for long loops, we have to consider winding loops. These may be regarded as loops that start at a point in the "original" sample but end at an equivalent point in a "copy" sample, arising from periodic boundary conditions. The copies cover all space. The probability for the loop reaching the equivalent point in the i-th nearest-neighbor copy at distance $r_i = n_i L$, is $P(i;\ell) = (2\pi\ell)^{-3/2}e^{-r_i^2/2\ell}$ in 3D. The number of copies which are i-th nearest neighbors scales as $4\pi(r_i/L)^2$ for large i. Thus the total probability for a winding loop starting at the origin to be of size ℓ is

$$p(\mathbf{0};\ell) \approx \sum_{i=0}^{\infty} 4\pi n_i^2 \left(\frac{1}{2\pi\ell}\right)^{3/2} \exp\left[-\frac{n_i^2 L^2}{2\ell}\right] \approx \frac{1}{L^3}\,, \quad (2)$$

after approximating the sum by an integral. We note that $p(\mathbf{0};\ell)$ is independent of ℓ and scales as L^{-3}. Summing over all possible initial points, the total probability to have a loop of size ℓ becomes

$$P_{3d}^{\rm w}(\ell) \approx \frac{1}{\ell}\sum_{\mathbf{x_o}} p(\mathbf{0};\ell) \sim \ell^{-1} \qquad (3)$$

independent of system size L. The crossover between the two behaviors occurs at the length scale $\ell_1 \sim L^2$, *i.e.* when the radius of gyration of a loop reaches the system size.

The average loop lengths $\langle\ell\rangle$ in both checkerboard and pyrochlore cases are finite. For the checkerboard, the PDF exponent τ_c being larger than 2 ensures a non-diverging $\langle\ell\rangle_c$. With the approximation that $P_{2d}(\ell) \propto \ell^{-\tau_c}$ at all even ℓ starting from $\ell_{min} = 4$, one estimates

$$\langle\ell\rangle_c = \left(\sum_{\ell=4,\ell\in 2\mathbb{N}}^{+\infty} \ell.\ell^{-\tau_c} \Big/ \sum_{\ell=4,\ell\in 2\mathbb{N}}^{+\infty} \ell^{-\tau_c}\right) \approx 24.9\,, \quad (4)$$

very close to the numerically obtained average 24.68(3).

For the pyrochlore, the combination of non-winding ($P_{3d}^{\rm nw} \sim L^3\ell^{-5/2}$) and winding loops ($P_{3d}^{\rm w} \sim \ell^{-1}$) conspire to produce a remarkably large but finite average loop length: $\langle\ell\rangle_p = 227.5(5)$. Even though they increase $\langle\ell\rangle_p$ by an order of magnitude compared to the 2D model, winding loops do not manage to make it divergent.

Considering non-winding and winding loops separately, we find that the non-winding loop average saturates with L, to the value $\langle\ell\rangle_{\rm n.w.} = 14.34(4)$. (Eq. (4) adapted to the pyrochlore gives 15.3). The winding loops by themselves have a diverging average $\langle\ell\rangle_{\rm w} \sim L^3/\ln L$.

Concerning the probability for two sites to be on the same loop, we note that the number of spin pairs belonging to the same loop of length ℓ is $\frac{1}{2}\ell(\ell-1)\times P(\ell)$, while there is a total of $\frac{1}{2}N(N-1)$ pairs of spins in the system. The probability averaged over all pairs is thus

$$\overline{C(r)} \sim \int_6^{8\,L^3} \frac{\ell(\ell-1)}{N(N-1)}\,P_{3d}(\ell){\rm d}\ell \sim \mathcal{O}(L^0) \qquad (5)$$

The non-winding loop contribution to this integral vanishes at large L, but the winding loop contribution leads to a constant term $C_\infty = C(r\to\infty)$ (Fig. 3). Indeed, we note that there will be several loops in a large system, each of which contains a finite fraction, f_i, of all sites. (We found $f_0 \approx 0.41, f_1 \approx 0.30, f_2 \approx 0.12\ldots$).

The 'scaling function' displayed in Fig. 2 shows that in 3D, there are in fact two length scales, namely when the radius of gyration hits the system size, $l_1 \sim L^2$, and when the loop explores the full volume, $l_2 \sim L^3$. The behaviour for $l > l_1$ obviously is influenced by the nature of the boundary conditions, e.g. the loops winding many times can break up into several loops terminating on the surface when open boundaries are considered.

For 2D, we note an intriguing similarity to the geometry of percolation hulls, which have a size distribution scaling with the same exponent we find above [20]. This we can rationalise as follows. Our loops can be thought of as defining a specific percolation problem, with checkerboard lattice sites painted in either colour with probability $p = 1/2$. It has been argued that neither short-range nor sufficiently rapidly decaying algebraic correlations between the occupied bonds influence the percolation critical exponents [21]. The 2D spin ice correlations indeed decay sufficiently fast, as r^{-2}. An additional feature of our loop ensemble is that loops of the same colour cannot cross or branch. From this it follows that each loop is at the same time a hull, whose length/perimeter should scale as $L^{7/4}$ (Fig. 2).

Worms: We now address properties of the worms. These are efficiently evaluated as our Monte-Carlo algorithm is in fact based on constructing worms, as flipping all spins in a worm conserves the ice-rules. Because worms can retrace parts of their path, their actual length can be longer than the system size. We therefore look at the distribution $Q(X)$ of the number of spins flipped during a worm update (Fig. 4), i.e., the number of sites visited by the worm an odd number of times. Again, two regimes appear in 3D, an $\ell^{-3/2}$ behavior (numerical exponent -1.48(4)) for $\ell \lesssim \ell_1$, and a ℓ-independent region for larger ℓ. These ($-3/2$ and 0) are random-walk exponents that can be derived similarly as in the loop case, Eqs. (1) and (3). The exponents for $Q(X)$ are shifted from the loop $P(\ell)$ exponents ($-5/2$ and -1) by 1; indeed if one asked the question "How long is the loop on which a randomly chosen spin sits ?", one would also get exponents $-3/2$ and 0.

The winding worm regime implies that 3D worms on average visit a finite fraction of the system size ($\approx 15\%$). Hence, a worm algorithm where a Monte Carlo update is

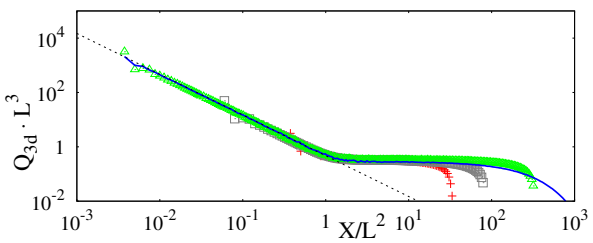

FIG. 4: Data points: probability distribution of number of spins flipped by worms ($L = 4$, 10, 40). Solid line: probability distribution of full worm length ($L = 40$) which weighs each site by the number of times it has been visited. This departs parametrically only for the longest worms, where multiple visits to a site become appreciable.

made by flipping the spins in a worm only requires a finite (typically 5−10) *constant* number of worms to decorrelate the system in 3D, *independent* of system size L, while the different behaviour of winding worms in 2D requires an increasing number of worm updates for decorrelation with L.

Conceptual and experimental implications: For both 2D and 3D, we have recovered exponents originally derived for systems *without* ice rules. The divergence-free conditions of Coulomb phases seem to have little effect on the 'universal' loop and worm statistics we have considered, which was not *a priori* to be expected, as the ice-rules impose algebraic spin correlations.

In the context of spin ice, worm statistics plays an important conceptual role as worms describe the tension-free (emergent) flux loops which are characteristic of the Coulomb phase. Here we have shown that their statistics resembles that of an ideal chain. Since, in a magnetic field, the worms have been utilised as an experimental diagnostic of Coulomb phase physics [18], a more detailed study of their statistics as a function of field strength would be worthwhile.

Regarding the loops, these are most naturally probed as a non-local correlation function. For instance, for a system of electrons which can hop only along a loop, the existence of the winding loops shows up in conductivity properties, as we will discuss elsewhere [15].

To the best of our knowledge, our loops first appeared in Villain's seminal paper in the context of a model of pyrochlore Heisenberg magnets with two species of magnetic ions [12–14]. Villain already noted the possibility of two (recurrent and transient) loop populations, which also show up for cosmic strings [5, 6] and laser speckles [8].

In Villain's model, each loop has a distinct colour encoding the direction of its Heisenberg spin (which is continuously variable and hence the number of colours is infinite), and spins are correlated only if they belong to the same loop. A finite value of C_∞ thus implies long-range spin order. Here we comment on two noteworthy features. Firstly the presence of several loops of size $\mathcal{O}(L^3)$ implies coexistence of several spatially intertwined but independent populations of long-range ordered spins. Secondly, a short-range interacting classical spin Hamiltonian of the kind envisaged by Villain allows gapless excitations for the Heisenberg spins. Thermal fluctuations out of this set of states could lead to locking of these populations into a more conventional collinear ordered structure. This is clearly a productive field for more detailed studies.

If one assigns a weight to each loop reflecting the number of flavours, n, it can take (which is not what is done in Villain's model, whose colours are used to distinguish the loops, not to weigh them), it becomes more favourable to have many, short loops as n grows. There is an extended literature on loop models, with some 3D work [22, 23], from which it is known that a phase transition results. In our case, an $n = \infty$ state is the "hexagonal protectorate" loop crystal proposed in the context of magnetodistortive phase transitions in the spinel compound $ZnCr_2O_4$ [24]. This has *only* loops of length 6 and breaks lattice translation symmetry.

In summary, we have presented an analysis of a set of extended degrees of freedom arising in an exotic phase of a three-dimensional magnet. This we hope will be of dual interest both from a statistical mechanics and a magnetic materials relaxation perspective. Further studies of these models, *e.g.* a quantum version thereof, are ongoing [25].

Acknowledgments − We thank John Chalker, Chris Henley and Vincent Pasquier for useful discussions.

[1] B. Duplantier, Phys. Rev. Lett. **81**, 5489 (1998).
[2] W. Werner, in *Random planar curves and Schramm-Loewner evolutions* (Springer, 2004), Chap. 2.
[3] J. L. Jacobsen and J. Kondev, Nucl. Phys. B **532**, 635 (1998).
[4] P. G. de Gennes, *Scaling concepts in polymer physics* (Cornell Univ. Press, Ithaca, 1979).
[5] T. Vachaspati and A. Vilenkin, Phys. Rev, D **30**, 2036 (1984).
[6] D. Austin, E. J. Copeland, and R. J. Rivers, Phys. Rev, D **49**, 4089 (1994).
[7] M. Viret *et al.*, Phys. Rev. Lett. **93**, 217402 (2004).
[8] K. O'Holleran, M. R. Dennis, F. Flossmann and M. J. Padgett, Phys. Rev. Lett. **100**, 053902 (2008).
[9] S. T. Bramwell, and M. J. P. Gingras, Science **294**, 1495 (2001).
[10] S. V. Isakov, K. Gregor, R. Moessner, and S. L. Sondhi, Phys. Rev. Lett. **93**, 167204 (2004).
[11] T. Fennell *et al.*, Science **326**, 415 (2009).
[12] C. L. Henley, Annual Review of Condensed Matter Physics **1**, 179 (2010).
[13] J. Villain, Zeitschrift Für Physik B **33**, 31 (1979).
[14] S. T. Banks, S. T. Bramwell, T. Fennell, M. J. Harris, unpublished.

[15] L. D. C. Jaubert, M. Haque, S. Pitaecki, and R. Moessner, in preparation (2011).
[16] G. T. Barkema and M. E. J. Newman, Phys. Rev. E **57**, 1155 (1998).
[17] C. Castelnovo, R. Moessner, and S. L. Sondhi, Nature **451**, 42 (2008).
[18] D. J. P. Morris *et al.*, Science **326**, 411 (2009).
[19] B. D. Hughes, *Random walks and random environments* (Oxford University Press, 1995).
[20] H. Saleur, and B. Duplantier, Phys. Rev. Lett. **58**, 2325 (1987).
[21] A. Weinrib, and B. I. Halperin, Phys. Rev. B **27**, 413 (1983).
[22] K. Shtengel and L. P. Chayes, J. Stat. Mech. P07006 (2005) and references therein.
[23] M. Ortuño, A. M. Somoza, and J. T. Chalker, Phys. Rev. Lett. **102**, 070603 (2009).
[24] S. H. Lee *et al.*, Nature **418**, 856 (2002).
[25] N. Shannon, private communication